Journal of Cell Science 107, 775-784 (1994)
Printed in Great Britain © The Company of Biologists Limited 1994

Quantification of microtubule dynamics in living plant cells using fluorescence redistribution after photobleaching

J. M. Hush*, P. Wadsworth, D. A. Callaham and P. K. Hepler†

Biology Department, University of Massachusetts, Amherst, MA 01003, USA

*Present address: School of Biological Sciences, University of Sydney, NSW 2006, Australia
†Author for correspondence

SUMMARY

Microtubule (MT) turnover within the four principal MT arrays, the cortical array, the preprophase band, the mitotic spindle and the phragmoplast, has been measured in living stamen hair cells of *Tradescantia* that have been injected with fluorescent neurotubulin. Using the combined techniques of confocal laser scanning microscopy and fluorescence redistribution after photobleaching (FRAP), we report that the half-time of turnover in spindle MTs is $t_{\frac{1}{2}}$=31±6 seconds, which is in excellent agreement with previous measurements of turnover in animal cell spindles. *Tradescantia* interphase MTs, however, exhibit turnover rates ($t_{\frac{1}{2}}$=67±seconds) that are some 3.4-fold faster than those measured in interphase mammalian cells, and thus are revealed as being highly dynamic. Preprophase band and phragmoplast MTs have turnover rates similar to those of interphase MTs in *Tradescantia*. The spatial and temporal aspects of the fluorescence redistribution after photobleaching in all four MT arrays are more consistent with subunit exchange by the mechanism of dynamic instability than treadmilling. This is the first quantification of MT dynamics in plant cells.

Key words: microtubule, *Tradescantia*, FRAP, cell division

INTRODUCTION

It has only recently become possible to analyze the spatial distribution and dynamics of all arrays of microtubules (MTs) in living plant cells. Zhang et al. (1990) first reported the successful application of fluorescent analogue cytochemistry to examine in vivo MT dynamics in plants, showing that mammalian neurotubulin, labelled with carboxyfluorescein (CF) and microinjected into living, dividing cells of *Tradescantia* stamen hairs, incorporates into endogenous MT polymers, allowing the examination of dynamic transitions of MT arrays through mitosis and cytokinesis. The close congruence in structure between images obtained in this as well as subsequent studies (Cleary et al., 1992; Zhang et al., 1993), with those previously shown by immunofluorescence microscopy (e.g. see Gunning, 1982; Wick, 1985; Palevitz, 1988), demonstrates that the injected brain tubulin acts as a faithful analogue of plant tubulin, and is therefore a useful probe to further investigate the dynamics of plant MTs in vivo. Particularly convincing evidence that confirms this is the work by Wasteneys et al. (1993) revealing the identical sensitivity of CF-tubulin-containing plant MTs and endogenous plant MTs to the herbicide oryzalin, which has high specificity for plant tubulin but no appreciable binding affinity to brain tubulin (Morejohn et al., 1987). Since MTs play critical roles in establishing cell polarity in plants (Hush et al., 1990; Hush and Overall, 1992), and in orchestrating plant cell division (for reviews, see Staiger and Lloyd, 1991; Hepler et al., 1993) it is important to understand their dynamic behavior.

Prior to this we have not had any quantitative information about the kinetics of MT turnover for interphase or mitotic arrays in plant cells. One approach that has been useful in analyzing MT dynamics in animal cells is the quantitative and sensitive technique of Fluorescence Redistribution After Photobleaching (FRAP; Axelrod et al., 1976), which allows measurement of steady-state MT dynamics in living cells (Saxton et al., 1984; Wadsworth and Salmon, 1986a,b; Sammak et al., 1987; Sammak and Borisy, 1988a; Lim et al., 1989). In a typical FRAP experiment, fluorescently labelled tubulin is microinjected into a living cell and allowed to equilibrate with the endogenous tubulin pool; a brief pulse of laser light is then used to irreversibly bleach the tubulin fluorophores in a localized region of the cell. The subsequent recovery of fluorescence is a measure of the turnover of unbleached fluorescently labelled tubulin subunits for bleached subunits. Interestingly, such studies on mammalian cells (e.g. see Saxton et al., 1984; Wadsworth and Salmon, 1986a,b) indicate that the exchange of tubulin subunits with MTs is about ten times faster in mitotic spindles than in interphase MT arrays.

In the present study, we have used the techniques of fluorescent analogue cytochemistry and FRAP to examine the dynamics of tubulin subunit exchange in MTs of the four different arrays that exist in plant cells: interphase, preprophase band (PPB), spindle and phragmoplast MTs, in *Tradescantia*

stamen hair cells. Our results indicate that the rates of spindle MT turnover are strikingly similar in plant and animal cells, but plant cell interphase MTs exhibit much higher (3.4-fold) turnover rates than those in animal cells. We also report that PPB and phragmoplast MTs appear to have identical dynamic properties to interphase MTs. These results are of significance in that they provide new insight into the molecular behavior of the different plant MT arrays, especially as they compare with the previously determined MT turnover rates in animal cells. This is the first report of MT turnover kinetics in plant cells.

MATERIALS AND METHODS

Cell culture

Stamen hairs were dissected from buds of *Tradescantia virginiana* inflorescences and immobilized on the surface of a coverslip using a thin film of low-temperature-gelling agarose (Sigma, type VII, 1%, in 0.02% Triton X-100). The bathing medium contained 5 mM HEPES, 5 mM KCl, 0.1 mM $CaCl_2$, adjusted to pH 7.0 with KOH.

Tubulin purification and CF-labelling

Pig neurotubulin was purified by two cycles of temperature-dependent assembly and disassembly, followed by phosphocellulose chromatography. Fluorescent labelling of tubulin was achieved by the following method (see Wadsworth and Salmon, 1986c; Hyman et al., 1991): phosphocellulose-purified tubulin was polymerized at a concentration of 3.5 mg/ml at 37°C for 30 minutes, in a buffer containing 4 M glycerol, 10 mM $MgSO_4$, 2 mM EGTA, 1 mM GTP, 80 mM PIPES at pH 6.9. 5-(and -6-)-carboxyfluorescein succinimidyl ester (Molecular Probes) was dissolved in approximately 0.5 ml of dry DMSO and mixed rapidly with the protein at a 40:1 molar ratio (dye:tubulin), incubated at 37°C for 15 minutes in the dark. The reaction was quenched by adding sodium glutamate to a final concentration of 10 mM. The dye-protein mixture was then centrifuged at 100,000 ***g*** at 25°C for 90 minutes, over small sucrose cushions (40% sucrose, 10 mM $MgSO_4$, 2 mM EGTA, 80 mM PIPES) to collect the CF-labelled MTs; assembly-competent tubulin was further purified by 2 cycles of temperature-dependent polymerization in glutamate buffer (1 M sodium glutamate, 1 mM EGTA, 0.5 mM $MgSO_4$, 0.2 mM GTP, pH 6.9). The final MT pellet was resuspended in injection buffer (20 mM sodium glutamate, 0.5 mM $MgSO_4$, 1.0 mM EGTA, pH 6.9) and small samples were drop frozen in liquid nitrogen and stored at –80°C.

The dye:protein ratio of the tubulin prepared for the present study was 1.8:1, which is higher than usually attained by this method (see Hyman et al., 1991). Prior to use, CF-labelled tubulin was diluted with injection buffer to a final concentration of 0.1 mg/ml, and GTP added to a final concentration of 1.0 mM.

Microinjection procedure

Pressure injection of fluorescently labelled tubulin in *Tradescantia* cells was performed on an inverted Zeiss microscope (IM-35), using the procedure described by Zhang et al. (1990).

Confocal laser scanning microscopy (CLSM) and photobleaching

Approximately 10 to 20 minutes following microinjection of CF-tubulin, MTs were imaged on a Bio-Rad MRC600 confocal laser scanning microscope, coupled to a Nikon Optiphot microscope. A high numerical aperture oil-immersion objective (Nikon ×40, 1.3 NA) was used to maximize the collection of the emitted fluorescent light. During image acquisition, neutral density filters were used to reduce the power of the 10 mW argon ion laser excitation light (488 nm) to approximately 3.1 nW, to minimize photodamage to the cell and photobleaching of the fluorophore. The adjustable confocal aperture was opened to position 5 for two reasons: first, to increase the depth of field so that minor fluctuations in the focus during image acquisition would not erroneously contribute to the signal; and second, to increase the emitted light signal permitting short exposure times. Images were collected as Kalman averages of 1-3 scans. Laser power was measured using a photodiode (Hamamatsu, cat no. S-1133-01), connected to a circuit that amplifies the photocurrent and converts it to a voltage, that was measured with a multimeter. The photodiode was attached to the undersurface of a coverslip and positioned at the stage of the microscope, and voltage measurements were taken in scanning or bleaching mode of the CLSM, employing the same objective and confocal settings as those used in experiments. Using a ×40 objective, the diameter of the laser beam at the microscope stage is approximately 3.1 μm, thus the laser intensity at the specimen in the scanning mode is approximately 400 W m^{-2}.

Prebleach images were first obtained using the normal image acquisition mode on the CLSM. One minute later, an area of MTs, approximately 10 μm^2, was photobleached using a laser intensity of 16 kW m^{-2} for 3 seconds (interphase MTs) or 1-2 seconds (PPB, spindle and phragmoplast MT arrays), using the 'bleach' function on the MRC600. Images were automatically acquired using the 'time series' program at approximately 3, 11, 21, 30, 39, 49, 58, 68, 78, 87, 118, 178, 269, 329 seconds after bleaching.

Data analysis of FRAP experiments

For analysis, the average pixel intensity of the photobleached region and the whole MT array in each case, was measured from the original stored image, using the 'histogram' function on the CLSM. For each image, the ratio of the average pixel intensity of the bleached region to the average pixel intensity of the whole array, was calculated. This method takes into account the slight photobleaching that occurs during the collection of images. The prebleach ratio was normalized to 1.0 and subsequent values were calculated as fractions of the prebleach value (after Olmsted et al., 1989). The means and standard errors of normalized ratios from different cells at successive time points were then used to describe the redistribution of fluorescence after photobleaching, for each of the different MT arrays. Generally, a cell was only used once for a FRAP experiment. However, in some cases where the cell progressed from one stage of the cell cycle to the next (e.g. anaphase to cytokinesis), and fluorescence was still bright, MTs were re-bleached (in a different area) and re-analyzed.

The exponential recovery of fluorescence in bleached regions of MTs was analyzed by using the following perturbation-relaxation equation:

$$F_{(t)} = F_0 + (F_\infty - F_0)\,(1 - e^{-kt}) \qquad (1)$$

after Salmon et al. (1984a). $F_{(t)}$ is the normalized fluorescence ratio at time t after photobleaching, and k is the first-order rate constant that describes the rate of recovery. F_0 is the fluorescence intensity measured immediately after bleaching (approx. 2 seconds), and F_∞ is the asymptotic value to which the fluorescence intensity recovers after bleaching. The first-order rate constant, k, was determined by fitting the function shown in equation (1) to the experimental data for each cell. The half-time ($t_{\frac{1}{2}}$) of recovery from F_0 to F_∞ was then calculated using the following equation:

$$t_{\frac{1}{2}} = \ln(2)/k\,. \qquad (2)$$

The mean half-time (± standard error of the mean, s.e.m., of n cells) was thus calculated for each type of MT array.

Photography

Photographs were taken of images (after brightness and contrast adjustments to match prebleach images) using a Polaroid Freeze Frame Video Recorder unit, with the Polaroid 35 mm adapter. Kodak T-Max 100 ASA film and T-Max developer was used for all photography.

RESULTS

Incorporation of microinjected CF-tubulin into *Tradescantia* MT arrays and CLSM imaging

CF-tubulin, once microinjected into the cytoplasm of *Tradescantia* cells, incorporates rapidly into endogenous MT polymers. An example of successful cytoplasmic loading of the tubulin analogue is shown in Fig. 1, where localization of the fluorescence (Fig. 1b) is confined to the cytoplasm, as viewed in the mid-plane of the cell (bright field image, Fig. 1a). Incorporation of the CF-tubulin into interphase MTs in this same cell, is shown in Fig. 1c, where the plane of focus has been shifted to the cell cortex.

Similarly, CF-tubulin was found to incorporate successfully into PPB, spindle and phragmoplast MT arrays, as has been shown previously in *Tradescantia* (Zhang et al., 1990), and can also be seen in Figs 2-6. The intracellular concentration of CF-tubulin protein in *Tradescantia* cells is estimated to be as low as 10 nM and thus is unlikely to affect the kinetics of MT polymerization in vivo. This estimation is based on the calculations of tubulin volume injected by Zhang et al. (1990), substituting the concentration of tubulin used in these experiments (0.1 mg/ml). It is evident from Figs 1-6 that there were negligible amounts of unbound dye in these cells (which might be present in the CF-tubulin solution, or result from degradation of the dye-tubulin complex), since no significant fluorescence was observed in intracellular compartments (e.g. vacuoles) or in adjacent cells, during the experimental period of observation (approx. 0.5 to 1.5 hours after microinjection).

Laser-scanning of cells during image acquisition did not detectably affect cell function in these experiments. Cytoplasmic streaming was observed to continue in all interphase cells, even after some 15-20 images had been collected. Mitotic cells generally proceeded through to the subsequent stage of division during, or after, the experimental period. However, cells injected during prophase often reverted back into interphase, making it difficult to label a PPB for FRAP experiments. The reversion of cells in prophase to interphase is not peculiar to these studies, since this phenomenon has been noted previously in both injected and non-injected stamen hair cells (Hepler, unpublished observations), and also in microinjected PtK_1 cells (Wadsworth, unpublished observations).

It is noteworthy that plant cells are particularly suitable for FRAP experiments using CLSM. Not only are plant cells better 'equipped' than animal cells to withstand laser irradiation (attenuated with neutral density filters), but confocal imaging is in fact necessary to elucidate MTs in one focal plane from out-of-focus fluorescence in other areas of these large, ovoid cells. Similar confocal imaging of animal cells injected with chromophores apparently causes rapid laser photodamage to the cells (Merdes et al., 1991; Shelden and Wadsworth, unpublished observations).

Fluorescence redistribution after photobleaching

Following bleaching of MTs that had incorporated CF-tubulin, a rapid recovery of fluorescence to approximately 90% of the original prebleach value has been observed in all experiments (Figs 2-6). Moreover, the pattern of fluorescence following recovery closely resembles the prebleach condition. In interphase cells (Fig. 2) the re-emergence of the original pattern is particularly striking, although due to limitations in resolution we are unable to say if the bright fluorescent lines represent single MTs or coaligned bundles (Sammak and Borisy, 1988b; Williamson, 1991). Despite this relatively clear visualization of linear fluorescent elements, MTs or MT bundles (Fig. 2), we hasten to add that the FRAP technique measures the behavior of a population of MTs. The resulting turnover thus reflects the contribution of growth and shrinking of individual MTs as well as the frequency of transitions between these two states.

Fluorescence micrographs from FRAP experiments for the various MT arrays in dividing stamen hair cells are shown in Figs 3-6. The PPB shown in Fig. 3 represents an early stage in its formation, since the band is reasonably wide and there are still a few cortical MTs outside of the band (Cleary et al., 1992). The plane of focus is such that the band, which is a continuous structure, appears in two sections; the right side has been bleached. Figs 4 and 5 are from metaphase and mid-anaphase cells, respectively. In Fig. 4a kinetochore bundle of MTs has been selectively bleached, while in Fig. 5 the bleached zone cuts across the proximal ends of a few kinetochore bundles, but also includes interzone MTs lying between the separating chromosomes.

The phragmoplast shown in Fig. 6 is at a relatively late stage of development as evidenced by its centrifugal growth close to the edges of the cell, by the appearance of a line demarking the emerging cell plate, and by the initiation of decay of the central MTs relative to those at the edges of the structure. In this instance the bleach zone is focused on an edge where MTs are highly structured (assembling vs disassembling) and where vesicle transport and aggregation continue to be active. In all of the examples shown in Figs 2-6 the cells are continuing their vital processes, which for Fig. 2 includes cytoplasmic streaming, and for the others includes notably the continuation of cell division. As a consequence, for example, chromosomes will exhibit positional changes between successive images in Fig. 4, or polar transport in Fig. 5. Finally, in Fig. 6 the processes of cell plate expansion occur during the time of inspection.

Recovery of fluorescence following photobleaching occurred uniformly throughout the bleached region; in no instance has there been evidence for translocation of the photobleached region (Figs 2-6). Note that in the case of the FRAP images of cortical MTs (Fig. 2), there are shifting regions of darker intensity in the background. As far as we could determine, none of these areas (other than the defined photobleached region) corresponds to translocation of the bleach zone; rather, they are likely to be the result of the background fluorescence in the streaming cytoplasm near the cell cortex, which contributes to the overall signal. The uniform recovery in the bleached zone over time, not only in the cortical array (Fig. 2), but in the other arrays as well (Figs 3-6), argues against fluorescent MTs outside of the bleached region shifting into the photobleached zone.

In the dividing cells we gave particular attention to the possibility of bleach migration in those instances in which the polarity of the MTs is well known; for example, the kinetochore bundle in Fig. 4 and the phragmoplast in Fig. 6. For the kinetochore the MTs would be unipolar with plus ends being attached to the chromosome at the upper edge of the bleached region. We also know from ultrastructural analyses of these cells that there are very few non-kinetochore MTs (Hepler, unpublished observations). Given these relatively favorable

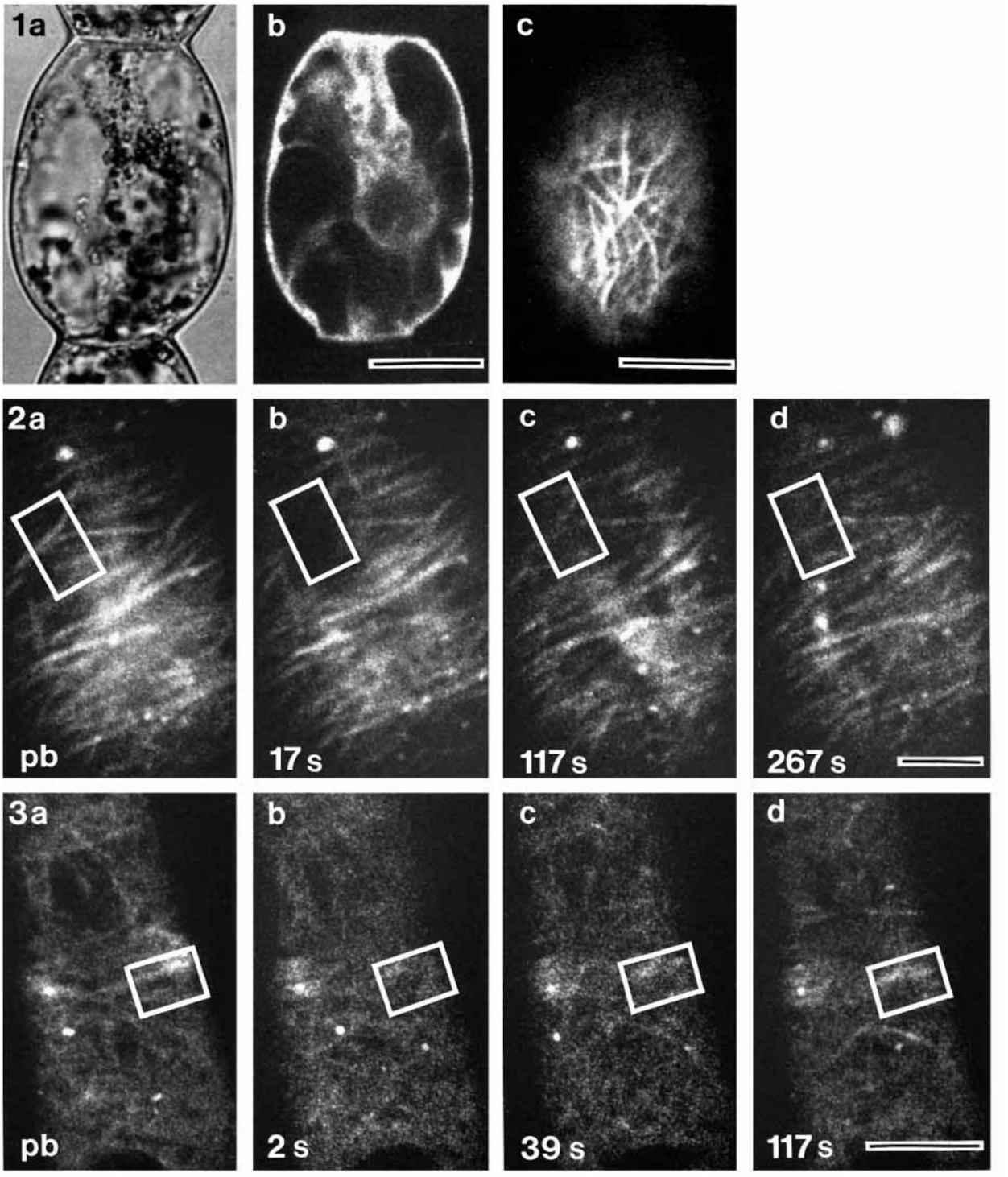

Fig. 1. Confocal laser scanning microscope (CLSM) images of a mature interphase *Tradescantia* stamen hair cell, showing a bright-field image of the cell (a) and fluorescence images of CF-tubulin, microinjected into the cytoplasm, as seen in the mid-plane of the cell (b) and following incorporation into interphase MTs in the cell cortex (c). Bars: 25 μm (a,b), 10 μm (c).

Fig. 2. CLSM images of fluorescence redistribution after photobleaching of interphase MTs in a *Tradescantia* stamen hair cell. Cells were photobleached for 3 seconds, at a laser intensity of approximately 16 kW m^{-2}. The bleached zone is outlined on each micrograph by a white box. Images before (prebleach, pb) and after photobleaching (time indicated in seconds) are shown. All images are Kalman averages of 3 scans. Bar, 5 μm.

Fig. 3. CLSM images of fluorescence redistribution after photobleaching of PPB MTs in a dividing *Tradescantia* stamen hair cell. Cells were photobleached for 1 to 3 seconds, at a laser intensity of approximately 16 kW m^{-2}. The bleached zone is outlined on each micrograph by a white box. Images before (prebleach, pb) and after photobleaching (time indicated in seconds) are shown. Images a and d are Kalman averages of 3 scans, while b and c are single scans. Bar, 10 μm.

viewing conditions we still do not detect a migration or directional flux in the recovery process. As was found in the phragmoplast, where the structure consists of overlapping arrays of MTs in which the plus ends are located in the mid-plane (Euteneuer and McIntosh, 1980), we also failed to observe a vectorial component to the recovery process.

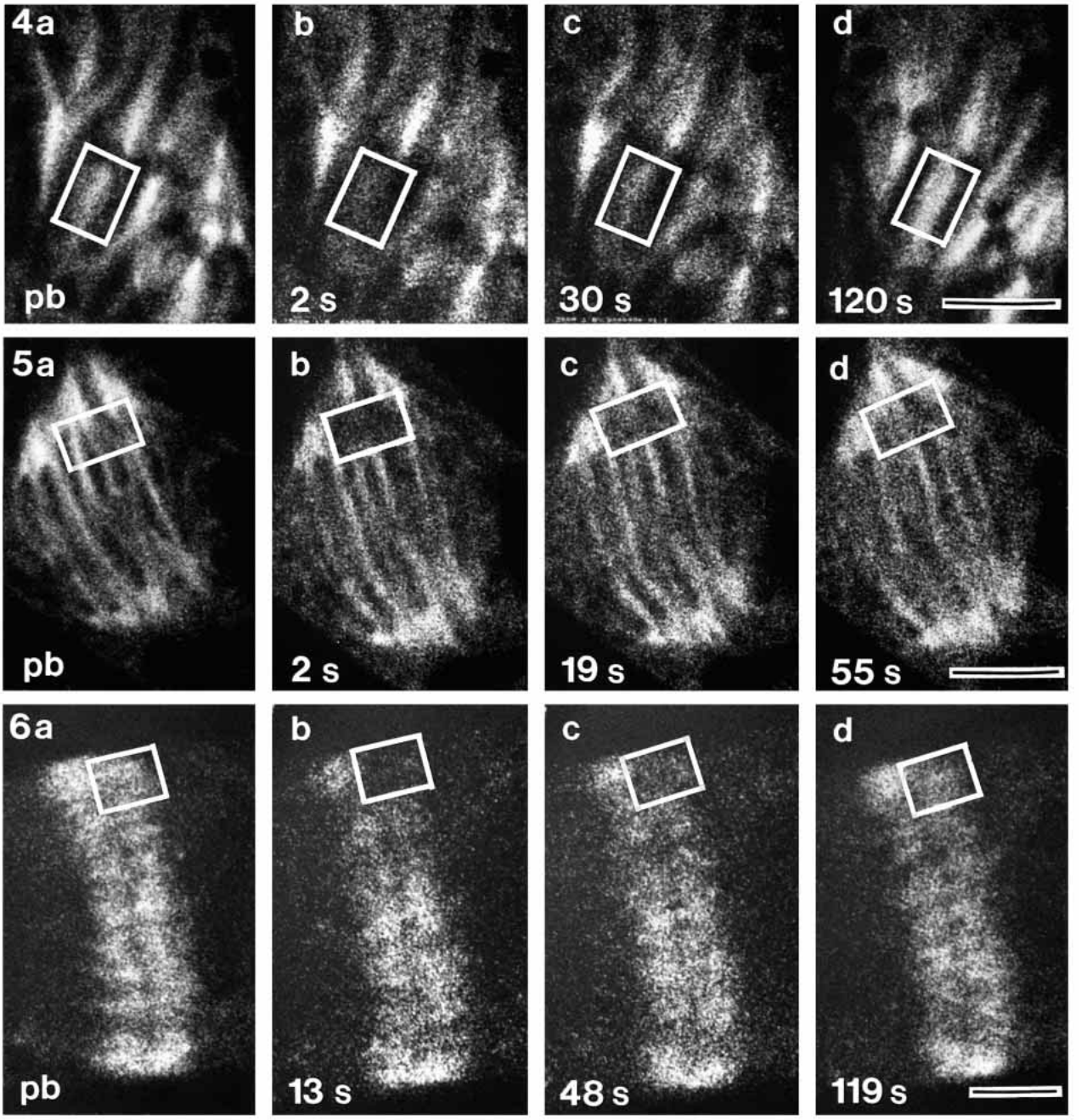

Fig. 4. CLSM images of fluorescence redistribution after photobleaching of kinetochore MTs in a *Tradescantia* stamen hair cell at metaphase. Cells were photobleached for 1 second, at a laser intensity of approximately 16 kW m^{-2}. The bleached zone is outlined on each micrograph by a white box. Images before (prebleach, pb) and after photobleaching (time indicated in seconds) are shown. a and b are Kalman averages of 3 scans, while c and d are single scans. Bar, 10 μm.

Fig. 5. CLSM images of fluorescence redistribution after photobleaching of kinetochore and interzone MTs in a *Tradescantia* stamen hair cell at anaphase. Cells were photobleached for 1 second, at a laser intensity of approximately 16 kW m^{-2}. The bleached zone is outlined on each micrograph by a white box. Images before (prebleach, pb) and after photobleaching (time indicated in seconds) are shown. a is a Kalman average of 3 scans, while b, c and d are single scans. Bar, 10 μm.

Fig. 6. CLSM images of fluorescence redistribution after photobleaching of phragmoplast MTs in a dividing *Tradescantia* stamen hair cell. Cells were photobleached for 1 second, at a laser intensity of approximately 15 kW m^{-2}. The bleached zone is outlined on each micrograph by a white box. Images before (prebleach, pb) and after photobleaching (time indicated in seconds) are shown. Images a and d are Kalman averages of 3 scans, while b and c are single scans. Bar, 5 μm.

In a control experiment, fluorescein-labelled bovine serum albumin (BSA) was injected (at a concentration of 1 mg/ml) into the cytoplasm of interphase *Tradescantia* cells, and the distribution of fluorescence recorded using CLSM before and after photobleaching for 6 seconds (using the same laser power and bleaching program for MT FRAP experiments). After laser irradiation for 3 seconds, a bleached zone was barely discernible at the earliest possible time of image acquisition, 2 seconds, and was undetectable in images taken at 11 seconds and after (data not shown). This demonstrates that recovery of the fluorescence of a soluble fluorescent protein occurs by rapid diffusion of the protein within the cytoplasm, agreeing with the theory that the half-time for recovery of fluorescence due solely to two-dimensional cytoplasmic diffusion, is approximated by:

$$t_{\frac{1}{2}} = \omega^2/4D, \quad (3)$$

where ω is the radius of a cylindrical bleached region and D is the diffusion coefficient (Axelrod et al., 1976). In this case, ω=3 μm and the diffusion coefficient of BSA in the cytoplasm is: 8.6×10^{-8} cm^2 s^{-1} (Salmon et al., 1984b), thus the $t_{\frac{1}{2}}$ for BSA diffusion is estimated to be 0.3 second. Therefore the slow redistribution of fluorescence, at least in interphase cells microinjected with fluorescein-tubulin, is not due to diffusion of CF-tubulin but to exchange of bleached subunits in MTs for CF-tubulin subunits in the cytoplasm.

Analysis of MT turnover kinetics

In all four MT arrays, the recovery of fluorescence approximately conformed to an exponential function of time after photobleaching (Fig. 7). However, the fit of the PPB MT data to this equation was not as good as for the other arrays, perhaps because this is a short-lived array and so variability between measurements may reflect different phases in the lifetime of the PPB. From the mean data points of fluorescence recovery for each MT type, it is clear that the irradiated areas of MT arrays were photobleached to about 40-50% of the prebleach level, and that in all instances the fluorescence recovered to between 85 and 95% of the original values.

The first-order rate constant (k) and half-time ($t_{\frac{1}{2}}$) of fluo-

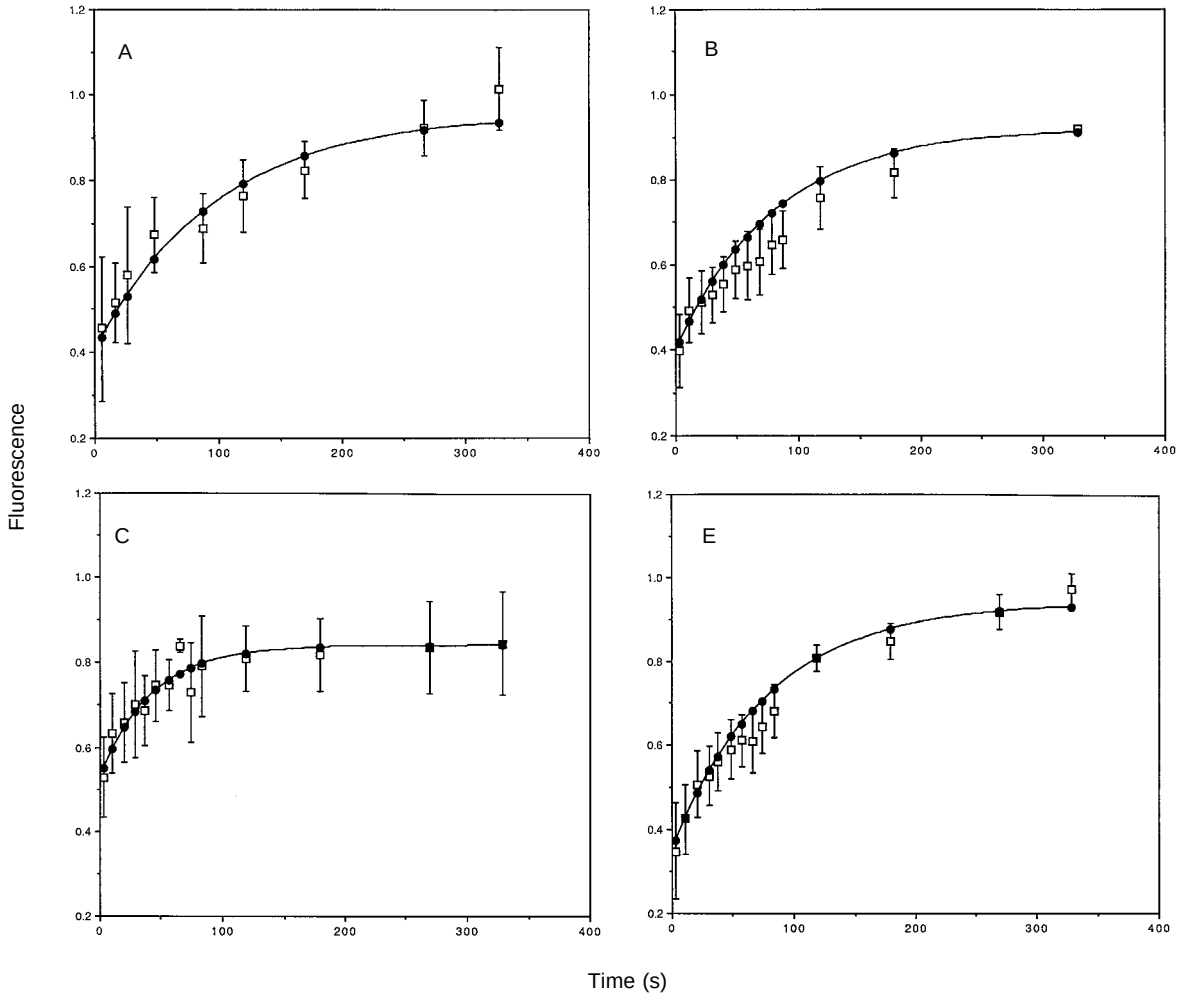

Fig. 7. Quantitative analysis of fluorescence recovery after photobleaching in interphase MTs (A), PPB MTs (B), spindle MTs (C) and phragmoplast MTs (D). Fluorescence values are expressed as fractions of the prebleach level, which is normalized to 1.0. Mean fluorescence values (open squares), ± s.e. of the mean, are plotted against time after photobleaching for n=5 cells (A), n=4 cells (B), n=3 cells (C) and n=6 cells (D). The theoretical exponential recovery is plotted on each graph (filled circles, and curve of best fit), using the mean values of k, F_0 and

Table 1. *Tradescantia* MT turnover: rate constants and half-times for different MT arrays, and comparison with animal cells.

	k/s^{-1} (±s.e.m.)	$t_{½}$/s (±s.e.m.)	*n*
Tradescantia			
Interphase	0.0104 (±0.001)	67.3 (±3.3)	5
Pre-prophase band	0.0124 (±0.002)	62.1 (±11.8)	4
Spindle	0.0237 (±0.004)	31.4 (±6.1)	3
Phragmoplast	0.0125 (±0.002)	60.0 (±8.1)	6
Animal Cells			
Interphase			
PtK_1*,¶	n.a.§	270 (±73)	4
BSC*,¶	n.a.	200 (±85)	17
Spindle			
sea urchin†	0.045	16 (±4.5)	12
sea urchin‡	0.06	19 (±6)	14
BSC*,¶	n.a.	13 (±7)	6
PtK_1*,¶	n.a.	11 (±6)	10
BSC§,‖	0.019	37	17
Newt lung§	0.008	87	n.a.

Tradescantia, sea urchin and newt lung cell measurements were made at room temperature. *Saxton et al. (1984); †Salmon et al. (1984); ‡Wadsworth and Salmon (1986a,b); §n.a., not available; ¶measured at 37°C; ‖measured at 32°C.

rescence recovery were determined for each cell, by fitting the data to an exponential perturbation-relaxation function (as described in Materials and Methods; see equations (1) and (2). Mean values of k and $t_{½}$ were calculated for each MT array, and the theoretical curve described by equation (1) is shown on each graph in Fig. 7, using mean values of K, F_0 and F_∞ in each case.

For comparison within the different plant MT arrays, and also between animal and plant cells, the mean values for the first-order rate constant and half-times of fluorescence recovery are listed in Table 1, along with relevant data from the literature. A striking result is that the half-time of MT turnover in *Tradescantia* spindles ($t_{½}$=31±6 seconds) is within the range of half-times that have been determined for mammalian, sea urchin and newt lung cell spindle MT turnover (Table 1). Equally of interest is the unexpected result that the kinetics of interphase MT turnover is much faster in plant cells ($t_{½}$)=67±3 seconds for *Tradescantia*) compared with mammalian cells ($t_{½}$=200-270 seconds; Saxton et al., 1984; Table 1).

PPB MTs appear to have similar dynamic properties to MTs of the cortical interphase array. Half-times of fluorescence recovery were: $t_{½}$=62±12 seconds (PPB) and $t_{½}$=67±3 seconds (interphase MTs). The kinetics of phragmoplast MT turnover ($t_{½}$=60±8 seconds) closely resembled those of interphase MTs and thus are distinguishable from the other truly mitotic MTs, the spindle apparatus, which exhibit markedly faster turnover rates ($t_{½}$=31±6 seconds).

DISCUSSION

The results demonstrate that plant MTs turn over rapidly. Specifically, we have shown that the rate of spindle MT turnover is remarkably similar in plant and animal cells, and that interphase, phragmoplast and PPB MTs exhibit kinetic properties that are slower than those of the mitotic apparatus, but dramatically faster than interphase MTs of animal cells. Even though a heterologous tubulin has been used as the probe, there seems ample reason to support the contention that the behavior of typical plant MTs is being observed. Not only is the neurotubulin incorporated into all the known arrays within the plant cell but in addition it yields morphological patterns closely similar to those established from numerous immunofluorescence studies (for reviews, see Lloyd, 1991). Finally, it has been determined that these fluorescent MTs disassemble in low concentrations of oryzalin (Wasteneys et al., 1993), thus displaying properties similar to plant MTs and quite dissimilar to MTs of animal origin.

FRAP, as a method to determine the kinetics and spatial aspects of MT turnover, has provided considerable valuable information in several systems; however, it has received criticism due to the possibility of laser-induced fragmentation of MTs. In our experiments, we used a laser intensity of approximately 16 kW m^{-2}, for an average of 2 seconds, for photobleaching, which is equivalent to 0.032 MJ m^{-2}. This is approximately 4,400-fold lower than the laser illumination reported by Vigers et al. (1988) to cause photodissolution (as observed by DIC microscopy) of fluorescently labelled MTs in vitro. Unfortunately, there are great difficulties associated with MT localization using immunofluorescence techniques in *Tradescantia* stamen hair cells, so it was not possible for us to check the integrity of photobleached MTs in this system by this method. But even so, we have shown here that the recovery of fluorescence in the interphase MT array of *Tradescantia* occurs by about 140 seconds in the *same* pattern as that observed prior to photobleaching, whereas if MTs are disassembled at low temperature, they re-assemble in completely different alignments at a far slower rate (i.e. polymers are not observed until about 6-10 minutes after cessation of the cold treatment; Hush, Huang, Callaham and Hepler, unpublished observations).

Others (Sammak et al., 1987) have clearly demonstrated that fibroblast cells fixed between 2.5 and 65 minutes after laser photobleaching at an estimated intensity of 50 MW m^{-2}, for 0.5 second, equivalent to 25 MJ m^{-2} (calculated from given bleach area of 4 μm × 57 μm and laser beam power of 13 mW) resulted in no discernible MT breakage as determined by tubulin immunofluorescence methods; these photobleaching conditions are 800-fold higher than those used in our experiments. Additionally, Saxton et al. (1984) have used both immunofluorescence and electron microscopy to show in BSC_1 interphase cells that there is no indication of MT fragmentation or distortion after photobleaching (at a laser power that we estimate to be 105 MJ m^{-2}). Finally, Okabe and Hirokawa (1993) have demonstrated that careful control of the extent of photobleaching (0.1 MJ m^{-2}) can safeguard against damage to MT structure or function. Taken together, these considerations, along with the observations that post-FRAP cells maintained unhindered mitosis and cytokinesis, suggest that the conditions of laser photobleaching used in our FRAP experiments did not result in photodissolution of MTs.

From our investigations of fluorescence recovery after photobleaching in *Tradescantia* cells, we were greatly interested to find that the rate of spindle MT turnover ($t_{½}$=31 seconds) is within the range of values reported for spindle MT dynamics

in other species ($t_{\frac{1}{2}}$=11-87 seconds). Of the four different MT arrays in plant cells, the spindle apparatus is the one that has a clear animal cell counterpart and, therefore, it seems likely that they would have similar dynamic properties. A further point of interest here is that the turnover rates that have been determined by FRAP for mammalian spindles, primarily represent the rapid dynamics of non-kinetochore MTs, which are the major component of MTs in spindles of these cells (Wadsworth and Salmon, 1986a,b; Mitchison and Salmon, 1992). In *Tradescantia* stamen hairs, however, the rapid rate of FRAP reflects the turnover primarily of kinetochore MTs, possibly suggesting that they are more dynamic than their counterparts in mammalian cells.

Perhaps the most exciting result from these experiments is that FRAP half-times for interphase MTs are some 3.4-fold faster in plants than those in animal cells. Cortical MTs in plant cells are thus revealed to be highly dynamic structures with respect to their molecular behavior. One interpretation is that the role of interphase MTs as structural elements in wall-less animal cells may limit their capacity as highly dynamic polymers. Indeed, this concept is consistent with the demonstration that in neurones, where MTs are responsible for morphological stability, half-times for MT turnover (as determined by FRAP experiments) are very slow ($t_{\frac{1}{2}}$=26±17 minutes in 3-day-old cultured PC-12 cells; Lim et al., 1989), and become progressively slower as neuronal growth proceeds and mechanical stability increases (e.g. $t_{\frac{1}{2}}$=201±91 minutes for 14-day-old PC-12 cells; Lim et al., 1989). In contrast, mechanical integrity is conferred upon plant cells by the relatively rigid wall surrounding each cell, possibly allowing a greater flexibility in the kinetics of interphase MT turnover in plant cells than in animal cells. Such a capacity for rapid turnover may explain how dynamic re-orientations of whole, coaligned cortical MT arrays in plant cells can occur so quickly; for instance, during cellulose microfibril deposition (reviewed by Marchant, 1982), and in response to plant growth substances (reviewed by Williamson, 1991), applied electrical or mechanical fields (Hush and Overall, 1991) and wounding (Hush et al., 1990).

The observation that there was a clear difference between the half-times of spindle MT turnover ($t_{\frac{1}{2}}$=31±6 seconds) and that of phragmoplast MTs ($t_{\frac{1}{2}}$=60±8 seconds), is interesting, especially since other recent studies of living *Tradescantia* cells indicate that the interzone MTs of the spindle consolidate to give rise to the densely packed cylinder of MTs, forming the phragmoplast (Zhang et al., 1990, 1993). Thus, more rapid turnover kinetics of the phragmoplast MTs might have been predicted; nevertheless, with a half-time of 60 seconds, these MTs are still turning over with great rapidity, in agreement with the findings by Asada et al. (1991) that phragmoplast MTs rapidly incorporate exogenous tubulin. Furthermore, these results suggest that the kinetics of MT turnover within an array are more likely to be determined by factors other than the cytomorphological origin of the array.

Also of note was the finding that the half-times of PPB and interphase MT turnover were so similar. Although both interphase and PPB MTs are localized in the cortex, their roles as cytomorphological determinants are markedly different: interphase MTs are considered to direct cell shape and the direction of cell expansion, via interactions with cellulose microfibrils in the cell wall (for review, see Seagull, 1989), while PPB MTs play a role in predicting the plane of cell division in plant cells (Gunning, 1982; Wick, 1991). Although the precise mechanisms of these interactions have not yet been elucidated, one might have expected PPB MTs to have a faster turnover rate than interphase MTs, given that they form rapidly (within 11 minutes in *Tradescantia*) during the transition into prophase (Cleary et al., 1992), and are a highly transient array (Wick, 1991), disappearing just prior to nuclear envelope breakdown and spindle formation. None the less, their cortical location may dictate that PPB MTs behave dynamically, like cortical MTs.

In considering the factors that might be involved in the regulation of plant MT dynamics, one possibility would be changes in the state of phosphorylation of tubulin or MT-associated proteins. For example, the cell cycle protein $p34^{cdc2}$ kinase, which occurs in higher plants (John et al., 1989; Feiler and Jacobs, 1990), peaks in activity during mitosis, but decreases before cytokinesis and remains low during interphase (Nurse, 1990). Therefore, it is possible that the increased activity of $p34^{cdc2}$ kinase at metaphase causes the more rapid turnover of spindle MTs, and that the slower dynamics of the PPB, phragmoplast and interphase MTs are in turn brought about by the lowered $p34^{cdc2}$ kinase activity at these stages of the cell cycle. Indeed, Verde et al. (1990) have shown that the addition of cdc2 kinase to interphase extracts from *Xenopus* eggs, alters MT dynamics to resemble more closely those of mitotic MTs. It has recently been elucidated that specific cyclin molecules appear to be responsible for this altered MT behavior (Verde et al., 1992). Furthermore, Lamb et al. (1990) have shown a marked alteration in the organization of interphase MTs following the in vivo application of $p34^{cdc2}$ kinase in mammalian fibroblasts.

Finally, we consider the mechanisms of subunit turnover that could account for the exchange of the bleached subunits for unbleached, fluorescent tubulin dimers. It is clear from the half-times of fluorescence redistribution that the process is not limited by diffusion. Current theory proposes that subunit exchange with the MT polymer can occur in two ways at steady-state. The first of these is treadmilling (Margolis and Wilson, 1978), in which the net addition of subunits at the plus end of MTs is balanced by the net loss at the minus end (Bergen and Borisy, 1980), causing dimers to flow through the polymer. A prediction of this model is that the bleached region of subunits would be translocated towards the minus end of the polymer. If treadmilling occurred in spindle MTs, one would expect that the photobleached region would be translocated towards the spindle poles, where the negative ends of MTs are located (Euteneuer et al., 1982). No such translocation was detected in our experiments, in agreement with that previously reported for FRAP in spindles of mammalian, newt and sea urchin cells (Gorbsky et al., 1988; Salmon et al., 1984a; Saxton et al., 1984; Wadsworth and Salmon, 1986a,b).

More recently, however, Mitchison and coworkers, utilizing the technique of photoactivation of caged fluorescein-tubulin, have demonstrated a polewards flux (~0.5 μm/min) of kinetochore MTs in PtK_1 cells (Mitchison, 1989) and newt lung cells (Mitchison and Salmon, 1992) in vivo. It appears that this slower flux of the more stable kinetochore MTs was not previously detected by the photobleaching method due to the rapid recovery of fluorescence in the more numerous non-kinetochore MTs. In photoactivation experiments, it becomes

possible to detect the fluorescence of a subset of more stable MTs (e.g. kinetochore MTs) against the background of non-fluorescent, more dynamic MTs (Mitchison, 1989; Mitchison and Salmon, 1992). In a complementary study, Sawin and Mitchison (1991) have distinguished that a rapid poleward flux (~3 μm/min) of spindle MTs occurs independently of kinetochores or kinetochore MTs in cell-free extracts from *Xenopus laevis* eggs. Thus, it is possible that in *Tradescantia* a slow poleward movement of a subset of MTs in the mitotic apparatus may be obscured by the rapid recovery of fluorescence in the majority of MTs in the bleached regions.

In the phragmoplast, MTs are organized into short, parallel arrays with the plus ends overlapping at the equator (Euteneuer and McIntosh, 1980). Asada et al. (1991) have demonstrated that MT polymerization occurs at the plus ends of phragmoplast MTs in vitro, and so the treadmilling model would predict the re-appearance of fluorescence after photobleaching at the equatorial region of the phragmoplast; however, this was not observed in our experiments. Thus, in the spindle, phragmoplast, as well as the PPB and interphase MTs, a uniform pattern of fluorescence recovery was observed after photobleaching, without any evidence for translocation of the bleach zone. Our results therefore do not provide evidence that treadmilling is the mechanism by which subunit exchange occurs for the majority of MTs in *Tradescantia*, but we acknowledge that the limitations in the spatial and temporal resolution of the system may have hindered detection of this. In this respect, it would be of great interest in future to apply the technique of photoactivation marking of plant MTs to investigate this question further.

The second process by which subunit exchange with MT polymers can occur is dynamic instability (Mitchison and Kirschner, 1984), where subunits are gained at the plus end during a growing phase and rapidly lost at the same end during a shrinking phase, such that whole MTs can turn over rapidly in a population of MTs at steady-state. The very rapid MT elongation and depolymerization predicted by this model is in accord with the rapid rate of tubulin turnover measured in both mitotic and interphase MTs in living *Tradescantia* cells. Although we cannot detect individual MT dynamic instability in these experiments, our data are more consistent with this than any other current model for MT turnover.

To conclude, plant MTs turnover quickly, an observation that enlarges our understanding of the role of the MT cytoskeleton in cell division, growth and morphogenesis.

The authors thank Eric Shelden and Ed Basgall for their assistance in setting up command modes on the CLSM for FRAP experiments. We also thank Lukas Hepler for assistance in the preparation of the Figures. This research was funded by an NSF grant (MCB-93-04646) to P.W. and a USDA grant (91-37304-6832) to P.K.H. This research was also supported by an NSF grant (BBS-87-14235) to the Microscopy Facility at the University of Massachusetts. J.M.H. gratefully acknowledges support from a Fulbright Postdoctoral Fellowship.

REFERENCES

Asada, T., Sonobe, S. and Shibaoka, H. (1991). Microtubule translocation in the cytokinetic apparatus of cultured tobacco cells. *Nature* **350**, 238-240.

Axelrod, D., Koppel, D. E., Schlessinger, J., Elson, E. and Webb, W. W. (1976). Mobility measurements by analysis of fluorescence photobleaching recovery kinetics. *Biophys. J.* **16**, 1055-1069.

Bergen, L. G. and Borisy, G. G. (1980). Head to tail polymerization of microtubules in vitro. *J. Cell Biol.* **84**, 141-150.

Cleary, A. L., Gunning, B. E. S., Wasteneys, G. O. and Hepler, P. K. (1992). Microtubule and F-actin dynamics at the division site in living *Tradescantia* stamen hair cells. *J. Cell Sci.* **103**, 977-988.

Euteneuer, U. and McIntosh, J. R. (1980). Polarity of midbody and phragmoplast microtubules. *J. Cell Biol.* **87**, 509-515.

Euteneuer, U., Jackson, W. T. and McIntosh, J. R. (1982). Polarity of spindle microtubules in *Haemanthus* endosperm. *J. Cell Biol.* **94**, 653-664.

Feiler, H. S. and Jacobs, T. W.(1990). Cell division in higher plants: a cdc2 gene, its 34 kDa product and histone H1 kinase activity in pea. *Proc. Nat. Acad. Sci. USA* **87**, 5397-5401.

Gorbsky, G. J., Sammak, P. J. and Borisy, G. G. (1988). Microtubule dynamics and chromosome motion visualized in living anaphase cells. *J. Cell Biol.* **106**, 1185-1192.

Gunning, B. E. S. (1982). The cytokinetic apparatus: its development and spatial regulation. In *The Cytoskeleton in Plant Growth and Development* (ed. C. W. Lloyd), pp. 229-292. Academic Press, New York.

Hepler, P. K., Cleary, A. L., Gunning, B. E. S., Wadsworth, P., Wasteneys, G. O. and Zhang, D. H. (1993). Cytoskeletal dynamics in living plant cells. *Cell Biol. Int. Rep.* **17**, 127-142.

Hush, J. M., Overall, R. L. and Hawes, C. R. (1990). Microtubule re-orientation precedes cell polarity changes in wounded pea roots. *J. Cell Sci.* **96**, 47-61.

Hush, J. M. and Overall, R. L. (1991). Electrical and mechanical fields orient cortical MTs in higher plant tissues. *Cell Biol. Int. Rep.* **15**, 551-560.

Hush, J. M. and Overall, R. L. (1992). Re-orientation of cortical F-actin is not necessary for wound-induced microtubule re-orientation and cell polarity establishment. *Protoplasma* **169**, 97-106.

Hyman, A., Dreschel, D., Kellogg, D., Salser, S., Sawin, K., Steffen, P., Wordeman, L. and Mitchison, T. (1991). Preparation of modified tubulins. *Meth. Enzymol.* **196**, 478-485.

John, P. C. L., Sek, F. J. and Lee, M. G. (1989). A homologue of the cell cycle control protein $p34^{cdc2}$, participates in the division cycle of *Chlamydomonas* and a similar protein is detectable in higher plants and some remote taxa. *Plant Cell* **1**, 1185-1193.

Lamb, N. J. C., Fernandez, F., Watrin, A., Labbe, J.-C. and Cavadore, J.-C. (1990). Microinjection of $p34^{cdc2}$ kinase induces marked changes in cell shape, cytoskeletal organization, and chromatin structure in mammalian fibroblasts. *Cell* **60**, 151-165.

Lim, S.-S., Sammak, P. J. and Borisy, G. G. (1989). Progressive and spatially differentiated stability of microtubules in developing neuronal cells. *J. Cell Biol.* **109**, 253-263.

Lloyd, C. W. (1991). *The Cytoskeletal Basis of Plant Growth and Form.* Academic Press, London.

Marchant, H. J. (1982). The establishment of plant cell shape by microtubules. In *The Cytoskeleton in Plant Growth and Development* (ed. C. W. Lloyd), pp. 295-320. Academic Press, New York.

Margolis, R. L. and Wilson, L. (1978). Opposite end assembly and disassembly of microtubules at steady-state in vitro. *Cell* **13**, 1-8.

Merdes, A., Stelzer, E. H. K. and De Mey, J. (1991). The three-dimensional architecture of the mitotic spindle, analyzed by confocal fluorescence and electron microscopy. *J. Electron. Microsc. Tech.* **18**, 61-73.

Mitchison, T. and Kirschner, M. (1984). Dynamic instability of microtubule growth. *Nature* **312**, 237-242.

Mitchison, T. J. (1989). Polewards microtubule flux in the mitotic spindle: evidence from photoactivation of fluorescence. *J. Cell Biol.* **109**, 637-652.

Mitchison, T. J. and Salmon, E. D. (1992). Poleward kinetochore fiber movement occurs during both metaphase and anaphase-A in newt lung cell mitosis. *J. Cell Biol.* **119**, 569-582.

Morejohn, L. C., Bureau, T. E., Mole-Bajer, A. S. and Fosket. D. E. (1987). Oryzalin, a dinitroaniline herbicide, binds to plant tubulin and inhibits polymerization in vitro. *Planta* **172**, 252-264.

Nurse, P. (1990). Universal control mechanism regulating onset of M-phase. *Nature* **344**, 503-508.

Okabe, S. and Hirokawa, N. (1993). Do photobleached fluorescent microtubules move?: Re-evaluation of fluorescence laser photobleaching both in vitro and in growing *Xenopus* axon. *J. Cell Biol.* **120**, 1177-1186.

Olmsted, J. B., Stemple, D. L., Saxton, W. M., Neighbors, B. W. and McIntosh, J. R. (1989). Cell cycle-dependent changes in the dynamics of MAP2 and MAP4 in cultured cells. *J. Cell Biol.* **109**, 211-223.

Palevitz, B. A. (1988). Microtubular fir-trees in mitotic spindles of onion roots. *Protoplasma* **142**, 74-78.

Salmon, E. D., Leslie, R. J., Saxton, W. M., Karow, M. L. and McIntosh, J. R. (1984a). Spindle microtubule dynamics in sea urchin embryos: analysis using a fluorescein-labeled tubulin and measurements of fluorescence redistribution after laser photobleaching. *J. Cell Biol.* **99**, 2165-2174.

Salmon, E. D., Saxton, W., Leslie, R., Karow, M. L. and McIntosh, J. R. (1984b). Diffusion coefficient of fluorescein-labeled tubulin in the cytoplasm of embryonic cells of a sea urchin: video image analysis of fluorescence redistribution after photobleaching. *J. Cell Biol.* **99**, 2157-2164.

Sammak, P. J., Gorbsky, G. J. and Borisy, G. G. (1987). Microtubule dynamics in vivo: a test of mechanisms of turnover. *J. Cell Biol.* **104**, 395-405.

Sammak, P. J. and Borisy, G. G. (1988a). Direct observation of microtubule dynamics in living cells. *Nature* **332**, 724-726.

Sammak, P. J. and Borisy, G. G. (1988b). Detection of single fluorescent microtubules and methods for determining their dynamics in living cells. *Cell Motil. Cytoskel.* **10**, 237-245.

Sawin, K. E. and Mitchison, T. J. (1991). Poleward microtubule flux in mitotic spindles assembled in vitro. *J. Cell Biol.* **112**, 941-954.

Saxton, W. M., Stemple, D. L., Leslie, R. J., Salmon, E. D., Zavortink, M. and McIntosh, J. R. (1984). Tubulin dynamics in cultured mammalian cells. *J. Cell Biol.* **99**, 2175-2186.

Seagull, R. W. (1989). The plant cytoskeleton. *Crit. Rev. Plant Sci.* **8**, 131-167.

Staiger, C. J. and Lloyd, C. W. (1991). The plant cytoskeleton. *Curr. Opin. Cell Biol.* **3**, 33-42.

Verde, F., Labbe, J.-C., Doree, M. and Karsenti, E. (1990). Regulation of microtubule dynamics by cdc2 protein kinases in cell free extracts of *Xenopus* eggs. *Nature* **343**, 233-238.

Verde, F., Dogterom, M., Stelzer, E., Karsenti, E. and Leibler, S. (1992). Control of microtubule dynamics and length by cyclin A- and cyclin B-dependent kinases in *Xenopus* egg extracts. *J. Cell Biol.* **118**, 1097-1108.

Vigers, G. P. A., Cove, M. and McIntosh, J. R. (1988). Fluorescent microtubules break up under illumination. *J. Cell Biol.* **107**, 1011-1024.

Wadsworth, P. and Salmon, E. D. (1986a). Analysis of the treadmilling model during metaphase of mitosis using fluorescence redistribution after photobleaching. *J. Cell Biol.* **102**, 1032-1038.

Wadsworth, P. and Salmon, E. D. (1986b). Microtubule dynamics in mitotic spindles of living cells. *Ann. NY Acad. Sci.* **466**, 580-592.

Wadsworth, P. and Salmon, E. D. (1986c). Preparation and characterization of fluorescent analogs of tubulin. *Meth. Enzymol.* **134**, 519-528.

Wasteneys, G. O., Gunning, B. E. S. and Hepler, P. K. (1993). Microinjection of fluorescent brain tubulin reveals dynamic properties of cortical microtubules in living plant cells. *Cell Motil. Cytoskel.* **24**, 205-213.

Wick, S. M. (1985). Immunofluorescence microscopy of tubulin and microtubule arrays in plant cells. III. Transitions between mitotic, cytokinetic and interphase microtubule arrays. *Cell Biol. Int. Rep.* **9**, 357-371.

Wick, S. M. (1991). The preprophase band. In *The Cytoskeletal Basis of Plant Growth and Form* (ed. C. W. Lloyd), pp. 231-244. Academic Press, London.

Williamson, R. E. (1991). Orientation of cortical microtubules in interphase plant cells. *Int. Rev. Cytol.* **129**, 135-206.

Zhang, D., Wadsworth, P. and Hepler, P. K. (1990). Microtubule dynamics in living dividing plant cells: confocal imaging of microinjected fluorescent brain tubulin. *Proc. Nat. Acad. Sci. USA* **87**, 8820-8824.

Zhang, D., Wadsworth, P. and Hepler, P. K. (1993). Dynamics of microfilaments are similar, but distinct from microtubules during cytokinesis in living, dividing plant cells. *Cell Motil. Cytoskel.* **24**, 151-155.

(Received 2 August 1993 - Accepted, in revised form, 14 December 1993)